Numerical Study of Carbon Nanotube Infra-Red Photo-Detectors

M. Pourfath and H. Kosina
Institute for Microelectronics, TU Wien
Gusshausstrasse 27–29/E360, A-1040 Vienna, Austria
Email: {pourfath|kosina}@iue.tuwien.ac.at

***Abstract*—Carbon nanotubes have been considered in recent years for future opto-electronic applications because of their direct band-gap and the tunability of the band-gap with the tube diameter. The numerical challenges for the analysis of carbon nanotube based photo-detectors are studied. The performance of infra-red photo-detectors based on carbon nanotube field-effect transistors is analyzed, using the non-equilibrium Green's function formalism. The relatively low ratio of the photo-current to the dark current limits the performance of such devices. We show that by employing a double gate structure this ratio can be significantly increased.**

Carbon nanotubes (CNTs) have been extensively studied in recent years due to their exceptional electronic, opto-electronic, and mechanical properties [1]. Some of the interesting electronic properties of CNTs are quasi-ballistic carrier transport [2, 3], suppression of short-channel effects due to one-dimensional electron transport [4], and a nearly symmetric structure of the conduction and valence bands, which is advantageous for complementary circuits. Moreover, owing to excellent optical properties of CNTs, an all-CNT electronic and opto-electronic circuit can be envisioned. The direct band-gap and its tunability with the CNT diameter renders them as suitable candidates for opto-electronic devices, especially for infra-red (IR) applications [5, 6] due to the relatively narrow band gap.

IR photo detectors based on carbon nanotube field effect transistors (CNT-FETs) have been reported in [5, 7, 8]. To explore the physics of such devices self-consistent quantum mechanical simulations have been performed. The performance of IR photo detectors based on CNT-FETs is analyzed numerically, employing the non-equilibrium Green's function formalism (NEGF). This method has been successfully utilized to investigate the characteristics of CNT-FETs [9–12]. To extend our previous work [13], we employed the NEGF method based on the tight-binding π-bond model to study quantum transport in IR photo detectors based on CNT-FETs and investigate methods to improve the performance of such devices.

The outline of the paper is as follows. In Section I, the NEGF formalism is briefly described. The implementation of this method for CNT-FETs is presented in Section II. In Section III single-gate and double-gate device responses are studied. Finally, conclusions are drawn in Section IV.

I. Non-equilibrium Green's Function Formalism

The NEGF formalism initiated by Schwinger, Kadanoff, and Baym allows to study the time evolution of a many-particle quantum system. Knowing the single-particle Green's functions of a given system, one may evaluate single-particle quantities such as carrier density and current. The many-particle information about the system is cast into self-energies, which are part of the equations of motion for the Green's functions. A perturbation expansion of the Green's functions is the key to approximate the self-energies. Green's functions enable a powerful technique to evaluate the properties of a many-body system both in thermodynamic equilibrium and non-equilibrium situations.

Four types of Green's functions are defined as the non-equilibrium statistical ensemble averages of the single particle correlation operator. The greater Green's function $G^{>}$ and the lesser Green's function $G^{<}$ deal with the statistics of carriers. The retarded Green's function G^{R} and the advanced Green's function G^{A} describe the dynamics of carriers. Under steady-state condition the equation of motion for the Green's functions can be written as [14]:

$$[E - H_0]\, G^{\mathrm{R,A}}(1,2) - \int d3\ \Sigma^{\mathrm{R,A}}(1,3) G^{\mathrm{r,a}}(3,2) = \delta_{1,2} \tag{1}$$

978-1-4244-1753-7/08/$25.00 ©2008 IEEE

$$G^{\lessgtr}(1,2) = \int d3 \int d4 \; G^{\mathrm{R}}(1,3)\Sigma^{\lessgtr}(3,4)G^{\mathrm{A}}(4,2) \tag{2}$$

The abbreviation $1 \equiv (\mathbf{r_1}, t_1)$ is used. H_0 is the single-particle Hamiltonian operator, and Σ^{R}, Σ^{A}, $\Sigma^{<}$, and $\Sigma^{>}$ are the retarded, advanced, lesser, and greater self-energies, respectively.

II. Implementation

This section describes the implementation of the outlined NEGF formalism for the numerical analysis of CNT-FETs. A tight-binding Hamiltonian is used to describe transport phenomena in CNT-FETs. The self-energy due to electron-photon interactions are studied next.

A. Tight-Binding Hamiltonian

In graphene three σ bonds hybridize in an sp^2 configuration, whereas the other $2p_z$ orbital, which is perpendicular to the graphene layer, forms π covalent bonds. The π energy bands are predominantly determining the solid state properties of graphene. Similar considerations hold for CNTs. We use a nearest-neighbor tight-binding π-bond model [9]. Each atom in an sp^2-coordinated CNT has three nearest neighbors, located $a_{\mathrm{cc}} = 1.42$ Å away. The band-structure consists of π-orbitals only, with the hopping parameter $t = V_{pp\pi} \approx -2.7$ eV and zero on-site potential.

B. Electron-Photon Self-Energies

The Hamiltonian of the electron-photon interaction can be written as [15–17]:

$$\hat{H}_{e-ph} = \sum_{l,m} M_{l,m} \left(\hat{b} e^{-i\omega t} + \hat{b}^{\dagger} e^{+i\omega t} \right) \hat{a}_l^{\dagger} \hat{a}_m \tag{3}$$

$$M_{l,m} = (z_m - z_l) \, \frac{i\mathrm{e}}{\hbar} \, \sqrt{\frac{\hbar I_\omega}{2N\omega\epsilon c}} \langle l | \hat{H}_0 | m \rangle \tag{4}$$

where z_m denotes the position of the carbon atom at site m, I_ω is the flux of photons with the frequency ω, and N is the photon number in the control volume. The incident light is assumed to be monochromatic, with polarization along the CNT axis, see Fig. 1.

We employed the lowest order self-energy of the electron-photon interaction [18]:

$$\Sigma^{<,\nu}_{l,m}(E) = \textstyle\sum_{p,q} M_{l,p} M_{q,m} \times \left[N G^{<,\nu}_{p,q}(E - \hbar\omega) + (N+1) G^{<,\nu}_{p,q}(E + \hbar\omega) \right] \tag{5}$$

where the first term corresponds to the excitation of an electron by the absorption of a photon and the second term corresponds to the emission of a photon by de-excitation of an electron. The transport equations must be iterated to achieve convergence of the electron-phonon self-energies, resulting in a self-consistent Born approximation. The greater self-energy is calculated similar to (5) and the retarded self-energy is given by

$$\Sigma^{\mathrm{r}}_{\mathrm{e-ph}}(E) = -\frac{i}{2}\Gamma_{\mathrm{e-ph}}(E) + \mathrm{P} \int \frac{dE'}{2\pi} \frac{\Gamma_{\mathrm{e-ph}}(E')}{E - E'} \; , \tag{6}$$

where $\Gamma_{\mathrm{e-ph}} \equiv i(\Sigma^{>}_{\mathrm{e-ph}} - \Sigma^{<}_{\mathrm{e-ph}})$ defines the broadening, and $\mathrm{P}\int$ represents the principal part of the integration. The imaginary part of the retarded self-energy broadens the density of states, whereas the real part shifts it in energy. It can be shown that the real part of the self-energy can be safely neglected [19].

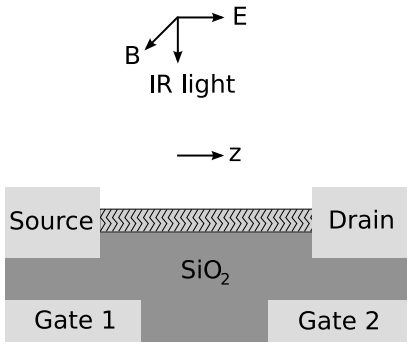

Fig. 1: The sketch of a double gate (DG) CNT-FET. $L_{\mathrm{G1}} = L_{\mathrm{G2}} = 10$ nm.

C. Non-locality of the self-energy

When scattering via a self-energy is introduced, the determination of the Green's function requires inversion of a matrix of huge rank. To reduce the computational cost, the *local scattering approximation* is frequently used [10, 18–22]. In this approximation the scattering self-energy terms are diagonal in coordinate representation. It allows one to employ the recursive algorithm for computing the Green's functions [18, 23]. The local approximation is well justified for electron-phonon scattering caused by deformation potential interaction [22]. However, we show that this approximation is not justified for electron-photon interaction.

For a device with a tube length of 12 nm the calculated photo current is shown in Fig. 2. The results are indicated as a function of the number of included off-diagonal elements of the retarded self-energy for electron-photon interaction. By including only the diagonal elements of the self-energy (local scattering approximation) the

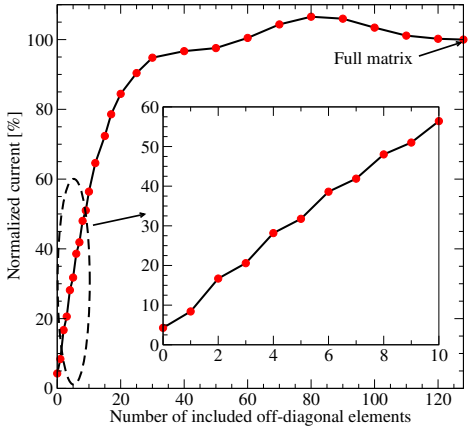

Fig. 2: The calculated photo-current as a function of the included off-diagonal elements of the retarded self-energy (Σ^{R}). The current is normalized to the value with full matrix elements. The full matrix size is 128×128.

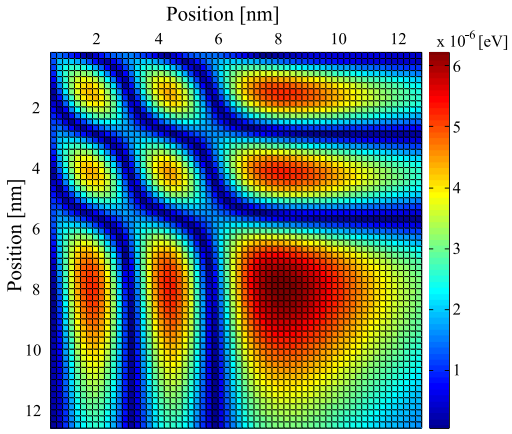

Fig. 3: The retarded self-energy (Σ^{R}) in coordinate representation for $E = 1.55$ eV. The existence of relatively strong off-diagonal elements indicate the non-locality of the interaction and the need to include the full matrix.

calculated current is only four percent of its value in the fully non-local case. This behavior can be well understood by considering the self-energy in two coordinate representation. As shown in Fig. 3 off-diagonal elements are relatively strong which indicate the need for a full matrix description. The oscillations in the self-energy result from the wave-like behavior in the quasi ballistic regime. This phenomenon is also present in Fig. 2. By increasing the number of included off-diagonal elements to around 50, the calculated photo-current increases. However, from this point the photo-current oscillates until it reaches its exact value at 128 off-diagonals. At some points the photo-current is even overestimated due to a change of the sign of the self-energy if the full matrix description is not employed.

III. Simulation Results

In a CNT-FET IR photo-detector incident photons generate electron-hole pairs and the electric field drives electrons and holes to the drain and source contacts, respectively. The photo-current at the source contact is mostly due to the drift of the photo-generated holes towards the source contact. However, there is a small reverse electron current due to tunneling of photo-generated electrons back to the source contact (Fig. 4-b).

Apart from the photo-current there is an un-wanted dark current due to thermionic emission and tunneling of carriers from the contacts to the channel. To reduce the dark-current we suggest a double gate (DG) structure (Fig. 1). We have previously shown that by employing a DG design, carrier injection at the source and drain contacts of a CNT-FET can be separately controlled [13]. Here, we extend our previous work and study a DG device for the detection of IR photons.

In a DG CNT-FET the band-edge profile near the contacts can be controlled by the gate voltages [13]. We consider the bias condition $V_{\mathrm{G1}} = V_{\mathrm{S}} - \Delta V$ and $V_{\mathrm{G2}} = V_{\mathrm{D}} + \Delta V$, where ΔV is some offset voltage. In a DG device, similar to a SG one, the electric field along the channel drives electrons towards the drain and holes towards the source contact. However, if $\Delta V > 0$ the local electric field close to the contacts reverses the sign, see Fig. 4. Under this condition the parasitic thermionic emission and tunneling of carriers from the contacts to the channel are strongly suppressed. As shown in Fig. 5, the parasitic dark-current decreases as ΔV increases. However, the dark-current increases again for $\Delta V > 0.1$ V because of the increase of the band to band tunneling current due to the increase of the electric field.

For $\Delta V > 0$ the local electric field drives photo-generated electrons and holes towards the source and drain contacts, respectively, which increases the reverse photo-current. As a result, as shown in Fig. 5, by increasing ΔV the total photo-current is slightly reduced, whereas the dark current is strongly suppressed. Our results indicate that for the given structure and drain voltage at $\Delta V \approx 0.07$ V the ratio of the photo-current to the dark-current can reach a maximum value of $I_{\mathrm{photo}}/I_{\mathrm{dark}} \approx 2 \times 10^5$, which implies a considerable improvement of the device characteristics.

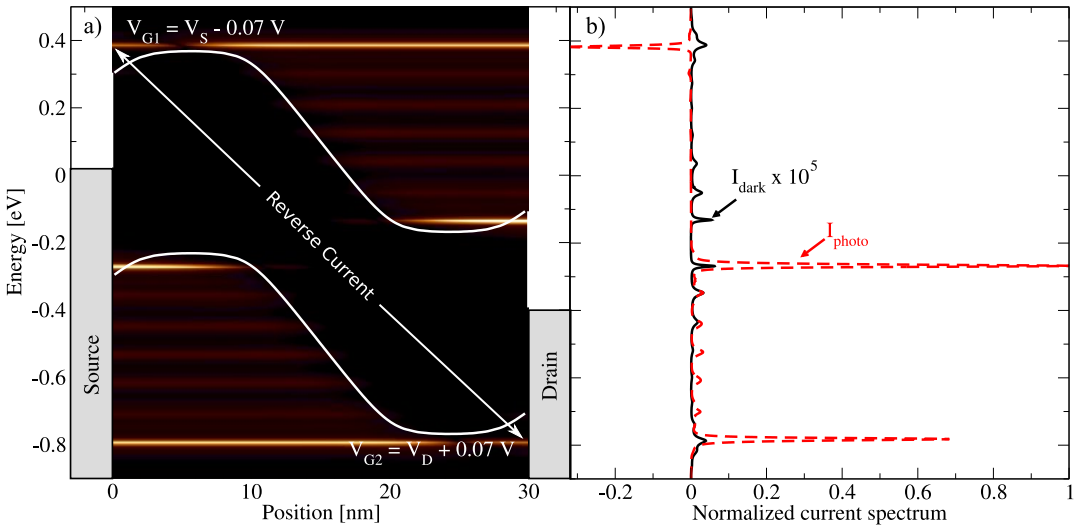

Fig. 4: a) The spectrum of the current along the channel of a DG CNT-FET. $\Delta V = 0.07$ V and $V_{\rm D} = 0.4$ V. b) The spectrum of the current at the source contact. The solid line shows the photo-current spectrum and the dashed line the dark-current spectrum which is scaled by a factor of 10^5.

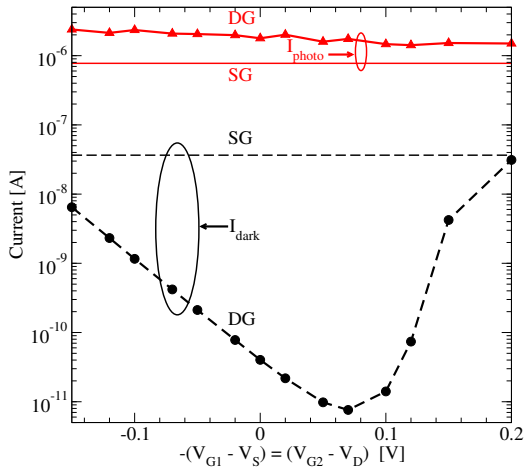

Fig. 5: The effect of the gate voltage offset ΔV on the photo-current and dark-current of a DG CNT-FET IR detector. Both the photo-current and the dark-current of a SG devices is shown for comparison.

IV. Conclusions

We present a numerical study of CNT-based photo-detectors employing the NEGF method. The results show that the local scattering approximation, which is widely used in quantum transport simulations, fails to predict the behavior of devices where electron-photon interaction is present. For accurate simulations a non-local self-energy must be taken into consideration. We show that the ratio of the photo-current to the dark-current can be considerably improved.

Acknowledgment

This work, as part of the European Science Foundation EUROCORES Programme FoNE, was supported by funds from FWF (Contract I79-N16), CNR, EPSRC and the EC Sixth Framework Programme, under Contract No. ERAS-CT-2003-980409.

References

[1] J. Appenzeller, Proc. IEEE **96**, 201 (2008).
[2] A. Javey *et al.*, Nature (London) **424**, 654 (2003).
[3] A. Javey *et al.*, Nano Lett. **4**, 1319 (2004).
[4] J.-Y. Park, Nanotechnology **18**, 095202 (2007).
[5] M. Freitag *et al.*, Nano Lett. **3**, 1067 (2003).
[6] M. Freitag *et al.*, Phys. Rev. Lett. **93**, 076803 (2004).
[7] S. Lu *et al.*, Nanotechnology **17**, 1843 (2006).
[8] J. Zhang *et al.*, Proc. SPIE **6395**, 63950A (2006).
[9] J. Guo *et al.*, Intl. J. Multiscale Comput. Eng. **2**, 257 (2004).
[10] A. Svizhenko *et al.*, Phys. Rev. B **72**, 085430 (2005).
[11] M. Pourfath *et al.*, IOP J. Phys.: Conf. Ser. **38**, 29 (2006).
[12] M. Pourfath *et al.*, Nanotechnology **18**, 424036 (2007).
[13] M. Pourfath *et al.*, J. Appl. Phys. **97**, 106103 (2005).
[14] S. Datta, Superlattices Microstruct. **28**, 253 (2000).
[15] E. Lindor *et al.*, J. Appl. Phys. **91**, 6273 (2002).
[16] D. A. Stewart *et al.*, Phys. Rev. Lett. **93**, 107401 (2004).
[17] D. A. Stewart *et al.*, Nano Lett. **5**, 219 (2005).
[18] R. Lake *et al.*, J. Appl. Phys. **81**, 7845 (1997).
[19] J. Guo, J. Appl. Phys. **98**, 063519 (2005).
[20] S. Datta, J. Phys.:Condensed Matter **2**, 8023 (1990).
[21] R. Lake *et al.*, Phys. Rev. B **45**, 6670 (1992).
[22] S. O. Koswatta *et al.*, IEEE Trans. Electron Devices **54**, 2339 (2007).
[23] A. Svizhenko *et al.*, J. Appl. Phys. **91**, 2343 (2002).